Black Sea Journal of Engineering and Science

INVESTIGATION OF USE OF HYDROCHARS OBTAINED FROM LEGUME WASTES AS FUEL AND THEIR CONVERSION INTO ACTIVATED CARBON FOR AMOXICILLIN REMOVAL

İsmail Cem KANTARLI[1]*

[1]*Ege University, Atatürk Medical Technology Vocational Training School, 35100, Izmir, Türkiye*

Abstract: Legume wastes, pinto bean peel (PBP) and pea shell (PS), were hydrothermally carbonized in subcritical water at various temperatures (200-240 °C) with the aim of obtaining a solid fuel, hydrochar. Fuel characteristics and chemical properties of hydrochars were determined by standard fuel analysis methods. Hydrochar yield decreased sharply with the increase of temperature due to the enhanced degradation of legume wastes. The weight percent of initial carbon in the legume wastes retained in the obtained hydrochars was lower than those in the literature due to the low hydrochar yields. The effect of temperature on carbon content and hence higher heating value (HHV) of hydrochar became noticable at 240°C. As a result of this effect, bituminous coal-like and lignite-like hydrochars with HHV of 31.2 and 28.1 MJ.kg^{-1} were obtained from PBP and PS, respectively. Hydrochars obtained at 220 °C were chemically activated with $ZnCl_2$ to produce activated carbons (PBP-AHC and PS-AHC). The activated carbons were characterized by elemental analysis, FTIR spectroscopy, BET surface area analysis and Scanning Electron Microscopy (SEM). BET surface area, total pore volume, and mesopore volume of PS-HC were determined as 1205 m^2. g^{-1}, 0.686 m^3. g^{-1} and 0.144 m^3. g^{-1}, respectively. PBP-AHC was found to have higher BET surface area (1350 m^2. g^{-1}), total pore volume (0.723 m^3. g^{-1}), and mesopore volume (0.249 m^3. g^{-1}) than PS-AHC. Activated carbons were tested as adsorbent for removal of amoxicillin (AMX) from aqueous solutions with the batch adsorption studies carried out at different initial concentrations, adsorbent dosage, and contact time. The compatibility of the adsorption data with the Langmuir and Freundlich isotherm models was checked to determine the adsorption capacity of activated carbons. The maximum Langmuir adsorption capacity (Q_{max}) was calculated as 188.7 and 70.9 mg. g^{-1} for PBP-AHC and PS-AHC, respectively. Adsorption kinetic analysis revealed that AMX adsorption on PBP-AHC and PS-AHC best fits with the pseudo-second order kinetic model. AMX adsorption was found to be faster on PBP-AHC than PS-AHC due to its higher surface area and more mesoporous character. $ZnCl_2$ activation of PBP-derived hydrochar produced a potential adsorbent for amoxicillin removal.

Keywords: Hydrochar, Activated carbon, Adsorption, Amoxicillin, Pinto bean peel, Pea shell

1. Introduction

Renewable energy is a fast growing energy sector and biomass is the only renewable energy source that can be used as a carbon-based fuel. However, the direct use of biomass as fuel is not economical due to its high pre-treatment cost, low energy density and low calorific value (Akogun and Waheed, 2019). In order for all kinds of biomass to be processed in the same combustion plant, they need to have a homogeneous structure and converting them into biochar would provide this condition. Two different thermochemical processes, dry and wet carbonization, are generally applied at low temperatures to transform biomass into stable, energy-intensive solid, biochar. With dry carbonization (DC), biomass is thermally decomposed in an inert gas atmosphere at low temperatures (200-300 °C) in short residence times (30-60 minutes). At the end of the process, biochar with a mass yield of 60-90% and an energy yield of 80-95% is obtained. Various studies exist in the literature which investigated the effects of parameters such as process temperature, heating rate and residence time on the mass yield, physicochemical properties and fuel properties of biochar obtained from different types of biomass (Yan et al., 2009; Ciolkosz and Wallace, 2011; Larsson et al., 2013; Satpathy et al., 2014). Production of biochar with DC of biomass with high water content is limited by the cost of pre-drying of the biomass. On the other hand, using wet carbonization method, also known as hydrothermal carbonization (HTC), it is possible to convert biomass containing up to 80% water to hydrochar, which has a higher energy density than biomass, under subcritical water conditions (usually in the temperature range of 180-260 °C, ambient pressure<22.1 MPa), under inert gas atmosphere and with short residence times without the need for drying. The resulting hydrochars have combustion characteristics and caloric values similar to lignite coal, and also better dewatering properties (Funke et al., 2013). Temperature

is the most effective process parameter in HTC. Residence time and the biomass: water ratio of the fed waste are the other parameters effective on the fuel characteristics of the produced hydrochar (Heilmann et al., 2010, 2011). Since water is a very good solvent under subcritical conditions, it can dissolve inorganic substances in biomass. Therefore, it is possible to obtain hydrochars with low ash content after HTC (Pala et al., 2014). Low ash content will reduce the tendency of hydrochars to cause problems such as fouling and slagging in combustion systems and will increase their preferability as a solid fuel. Dried legumes are used as a cheap protein and calorie source worldwide and especially in developing countries. Pinto bean (*Phaseolus vulgaris* L.) and pea (*Pisum sativum* Linn.) are the most widely grown legumes worldwide (Verma et al., 2011). They are also grown in abundance in Türkiye. The peel remaining after the separation of pinto bean (PBP) has a dietary fiber content of approximately 67% (Martínez-Castaño et al., 2020). It has been stated that the remaining part of the shell after the separation of pea grain (PS) has a dietary fiber content of approximately 50% and is a perishable waste (Mateos-Aparicio et al., 2010). PBP and PS to be used in the study are both lignocellulosic wastes and have high water content (~77%). These features make these wastes interesting as raw material for the production of solid fuel, hydrochar, by HTC. While there is no study on the HTC of PBP in the literature, only one study on the HTC of PS exist in the literature (Dong et al., 2019).

There are many studies in the literature on the production of activated carbon from different biomass/waste until today (Horikawa et al., 2010; Lim et al., 2010; Rashid et al., 2016; Limousy et al., 2017; Rodrigues et al., 2020; Yi et al., 2021). The common goal in these studies was generally to reduce the cost of activated carbon production. In the production of activated carbon from biomass, two methods are generally applied, namely chemical activation and physical activation. Physical activation method is applied in commercial activated carbon production (Yi et al., 2021). However, more studies on chemical activation exist in the literature due to its advantages such as lower process temperature, higher efficiency, more controllable pore formation and size compared to physical activation. In these studies, H_3PO_4, $ZnCl_2$ and alkali hydroxides were generally used as chemical activators (Limousy et al., 2017; Rodrigues et al., 2020; Rashid et al., 2016).

The properties required in activated carbon depend on its application area. For example, high mesoporosity is required for its usage as adsorbent in dye adsorption (Swan and Zaini, 2019), while surface functional groups are required for metal adsorption (Yang et al., 2019). It has been observed in the previous studies that pre-treatment of the biomass before activation improves the surface properties of the obtained activated carbon. It has been determined that the activation of biochar obtained by dry carbonization with strong acids forms carboxylic groups on its surface and increases the surface area due to its micropores (Hadjittofi et al., 2014; Qian et al., 2013; Iriarte-Velasco et al., 2016). For example, it was observed that the activation of biochar obtained from cactus fibers with HNO_3 increased the carboxyl groups on the surface, increasing the Cu^{2+} binding capacity (Hadjittofi et al., 2014). On the other hand, it has been reported that the activation of biochar obtained from glass wood with H_2O_2 increases the adsorption capacity of metal ions by increasing the cation exchange capacity due to the oxygenated groups on the surface (Huff and Lee, 2016). Similarly, activation of biochar with metal hydroxides has been observed to increase the adsorption capacity of metal ions by increasing the number of oxygenated groups, surface area and porosity in the obtained activated carbon (Petrovic´ et al., 2016; Goswami et al., 2016; Hamid et al., 2014). In the studies of Angin et al., activated carbons with a surface area of 1277 m^2 g^{-1} and a surface area of 801 m^2 g^{-1} were obtained from biochars activated with KOH, H_3PO_4 and $ZnCl_2$, and these active carbons has been effective in removing reactive dyestuffs from water (Angın et al., 2013a, 2013b).

In addition to biochars, hydrochar can also be used as raw material in the production of activated carbon. The difference of hydrochars from biochars is that they have less aromatic structure and generally more alkyl groups. A study by Sun et al. showed that hydrochars have the capacity to adsorb more amount of polar and non-polar organics than biochars (Sun et al., 2011). In some of the studies, hydrochars were directly used in the removal of dyestuffs (Parshetti et al., 2014; Flora et al., 2013), copper and cadmium (Regmi et al., 2012), and Pb^{2+} and Cd^{2+} (Elaigwu et al., 2014) from water. Studies focusing on the activation of hydrochars also exists in literature. Roman et al. found that the production of activated carbon with controlled surface chemistry and porosity from hydrochar can be achieved by physical activation with carbon dioxide (Roman et al., 2013). Pari et al also produced porous carbon spheres from hydrochars by chemical activation with KOH (Pari et al., 2014). Similarly, Laginhas et al. reported that a combination of HTC and $CaCO_3$ or K_2CO_3 activation can successfully produce activated carbon from chitosan (Laginhas et al., 2016). Sevilla and Fuertes reported that activated carbons with very high surface area can be produced by HTC of polysaccharide and wood powder followed by chemical activation with KOH (Sevilla and Fuertes, 2011).

Considering other studies on the production of activated carbon by chemical activation of hydrochars, it was found that NaOH activation of coconut shell hydrochar produced activated carbon suitable for cationic dye adsorption (Islam et al., 2017); $FeCl_3$ activation of *Salix psammophila* hydrochar produced activated carbon with high mesoporosity and a surface area of 349 $m^2.g^{-1}$ (Zhu et al., 2014); H_3PO_4 activation of orange peel hydrochar produced activated carbon with mesopore volume of 0.102 $cm^3.g^{-1}$ (Fernandez et al., 2015); NaOH activation of waste tea hydrochar produced activated carbon with mesopore volume of 0.21 $cm^3.g^{-1}$ and surface area of

368.92 $m^2.g^{-1}$ (Islam et al., 2015). Unlike the above studies, when wet carbonization of coconut shell in the presence of $ZnCl_2$ was performed, it was found that the mesopore volume increased by 67% (Jain et al., 2014). Eom et al., in his study, impregnated hydrochar obtained from brewed black tea waste at 200 °C for 12 hours with KOH in varying ratios of hydrochar: activating agent (between 1:2 and 1:4) and activated them at pyrolysis temperatures of 600 °C and 700 °C (Eom et al., 2021). As a result of activation, they have obtained active carbons with BET surface area varying in the 174 to 1398 $m^2.g^{-1}$ range and micropore volume varying in the 0.05 to 0.69 $cm^3.g^{-1}$ range. PBP and PS, which are the wastes to be used in this study with high water content (>77%), can be similarly evaluated as feedstock in the production of activated carbon with a two-step process.

Pharmaceutical compounds, especially antibiotics, are widely used in medical treatment of both humans and animals throughout the world and have emerged as a new class of pollutants. They bio-accumulate in the waters and pose a risk to the aquatic ecosystem, since they are released to water sources without being completely metabolized in the human/animal body and degrade very little after they are released (Yu et al., 2016; Garoma et al., 2010). Therefore, it is necessary to remove pharmaceutical substances from wastewater. Methods used for the removal of pharmaceuticals from wastewater include techniques such as ozonation, membrane filtration, photodegradation and biological treatment. The adsorption technique, which is more advantageous in terms of efficiency and cost compared to these techniques, is also frequently used for the removal of pharmaceutical substances from wastewater (Hayati et al., 2018). It is also stated in the literature that especially activated carbon adsorption is an effective approach in the removal of pharmaceuticals from wastewater (Redding et al., 2009). Amoxicillin (AMX) is a common penicillin-type antibiotic which is used in a wide spectrum against various bacteria in both human and veterinary medicine. It was reported to be present in surface water, domestic, industrial and hospital wastewater in concentration ranges of ng L^{-1} to mg L^{-1} (Elmolla and Chaudhuri, 2010; Zuccato et al., 2010; Serna-Galvis et al, 2017). As mentioned for pharmaceuticals removal above, adsorption process was reported to be more efficient than the other methods also for AMX removal. A number of studies exist in literature using different adsorbents including commercial granular activated carbon (De Franco et al., 2017), lignocellulosic waste based activated carbon (Pezoti et al., 2016; Laksaci et al., 2023; Limousy et al., 2017), carbon nanotubes (Balarak et al., 2016; Unutkan et al., 2018; Fazelirad et al., 2015), magnetic activated carbon (Saucier et al., 2017), magnetic graphene oxide (Moradi, 2015; Kerkez-Kuyumcu et al., 2016), metal-organic framework (Abazari and Mahjoub, 2018) and activated hydrochar (Ajala et al., 2023; Li et al., 2017). However, using activated hydrochar obtained from PBP and PS as adsorbent for AMX removal has not been studied before.

In this study, utilization of PBP and PS as energy feedstock and adsorbent was aimed by the application of a two-step process which followed the hydrothermal carbonization and chemical activation sequence. The aim of first step was to homogenize these wastes by converting them into hydrochars and to examine the feasibility of their direct use as fuel or use as precursor for activated carbon production. Variation of the fuel characteristics of derived hydrochars was investigated with respect to temperature. In the second step, feasibility of producing activated carbon from hydrochar by $ZnCl_2$ activation was investigated with the motivation of using it as adsorbent in treatment of wastewater streams. The chemical and morphological properties of activated hydrochars were compared according to the legume waste type. Additionally, AMX adsorption studies were carried out to check the potential of activated hydrochars as adsorbent and to examine the relation between their properties and AMX adsorption capacities.

2. Materials and Methods

2.1. Materials

All the chemicals and reagents used in this research were of analytical grade. The legume wastes, PBP and PS, were supplied by a local restaurant in Bornova, Izmir. PBP and PS had solid content of 19.6% and 22.9%, respectively. The legume wastes were dried at 60 °C overnight. Some properties of dried legume wastes were given in Table 1.

Table 1. Some properties of legume wastes

Legume waste	Proximate analysis, (dry basis, wt. %)				Ultimate analysis, (dry basis, wt. %)					HHV (MJ/kg)
	Volatile matter	Ash	Fixed carbon	Fuel ratio	C	H	N	S	O	
PBP	78.4	3.8	17.8	0.23	44.04	6.06	1.07	0.00	43.79	22.30
PS	77.5	5.0	17.5	0.23	43.39	5.75	4.19	0.02	42.85	21.41

HHV= higher heating value

As can be seen from Table 1, legume wastes have high volatile matter content and low fixed carbon content. High volatile matter contents of legume wastes is a disadvantage for their utilization as feedstock in existing gasification plants since it leads to tar formation (Maitlo et al., 2022). High volatile matter might cause a rapid and incomplete burning and hence emissions of high amount of pollutants such as CO, polycyclic aromatic

hydrocarbons, unburned products, etc. (Vassilev et al., 2015).

2.2. Hydrothermal Carbonization Experiments

A 0.5 L stainless steel autoclave with a magnetic stirrer was used for HTC experiments (Balmuk et al., 2023). Both heating and cooling system exists in the oven. A PID controller regulates and fixes the process temperature. It was observed in a previous study that HTC of biomass at temperature below 200 °C led to ineffective carbonization of biomass and produced hydrochar which had TG curve similar to that of biomass (Kantarli et al., 2016). Therefore, HTC experiments were performed at reaction temperature of 200, 220 and 240 °C at autogeneous pressure as duplicates. The heating rate was 5 °C. min⁻¹. The water: solid ratio was selected as 7: 1 in order to provide homogenous stirring of the mixture in autoclave reactor. 25 g of dried legume waste was mixed with 175 mL of distilled water. After loading the dried legume waste + water mixture to the reactor, the reactor was sealed. Next, the sealed reactor was purged with N_2 to remove the air inside, heated to the pre-determined temperature and held at this temperature for 60 min. At the end of 60 min., the reactor was cooled and the gaseous products were released to the atmosphere. The solid product, hydrochar, was seperated from aqueous phase by filtration of the slurry mixture inside the reactor. The hydrochar was washed with 100 mL water and dried at 105 ° C for 24 h. The dried hydrochar was weighed and the mass yield was calculated accordingly. Hydrochars were abbreviated in the order of "feedstock type-HC-temperature". For example, PBP-HC-200 corresponds to the hydrochar obtained from pinto bean peel at 200 °C for 60 min.

2.3. Chemical Activation of Hydrochars

Hydrochars derived from legume wastes, PBP-HC-220 and PS-HC-220, were chemically activated by $ZnCl_2$. $ZnCl_2$ activation experiments were done once without replications. $ZnCl_2$:precursor ratio was chosen as 1:1 in order to consume less chemical. As the first step of activation, $ZnCl_2$ solution was prepared by dissolving 10 g of $ZnCl_2$ in approximately 20 mL of water. 10 g of hydrochar was impregnated with the $ZnCl_2$ solution. The mixture was dried in an oven at 100 °C overnight. The dried mixture was loaded in a pyroysis reactor and activated at 500 °C under N_2 flow (100 mL/min) for 1 h. At the end of 1 h, the reactor was cooled. Then, the reactor residue was collected in a boiling flask, mixed with 150 mL of 10% HCl solution and refluxed for 1 h. Next, the mixture was filtered under vacuum. The acid treated solid residue separated from the mixture was washed with hot distilled water until no chloride ions was observed in filtrate. Finally, the activated hydrochar samples (PBP-AHC and PS-AHC) were dried at 100 °C for 24 h and sieved to the particle size <100 μm for AMX batch adsorption studies.

2.4. Analysis

The ash content and the volatile matter content of legume wastes and their hydrochars were determined according to the standard methods NREL/TP-510-42622 and ASTM D3175-89a, respectively. C, H, N, S content of legume wastes and their hydrochars were determined by a ELEMENTAR Vario Micro Cube Organic elemental analyzer. The higher heating value (HHV) of legume wastes and their hydrochars were calculated according to the Equation 1 given in the literature (Channiwala and Parikh, 2002), which is as follows (equation 1):

$$HHV, \left(\frac{MJ}{kg}\right) = 0.3491 * C + 1.1783 * H + 0.1005 * S - 0.1034 * O - 0.0151 * N - 0.0211 * Ash \quad (1)$$

C, H, O, N, S, and Ash correspond to the mass percentages of carbon, hydrogen, oxygen, nitrogen, sulphur, and ash in the sample, respectively.

The FTIR spectra of legume wastes, hydrochars and activated carbons were taken with ATR-FTIR spectrometer (Spectrum 100, PerkinElmer, Waltham, MA, USA). Brunauer, Emmett and Teller (BET) surface area and pore volume of activated carbons were analyzed by performing N_2 adsorption at 77 K (Micrometrics Gemini V). Degassing of activated carbon was carried out at 300 °C for a duration of 3 h before the measurement. The surface morphologies of legume wastes, hydrochars, and activated carbons were examined by Scanning Electron Microscope (SEM). A FEI QUANTA 250 FEG was used to take SEM images of samples at different magnitudes.

2.5. Adsorption Tests

The potential of activated hydrochars for AMX removal was checked with the batch adsorption studies carried out at different initial concentrations (75–250 mg.L⁻¹), times (5 min–1440 min) and activated carbon dosage (0.5–3 g.L⁻¹).

In each experiment, 25 mL of AMX solution was poured into a 50 mL flask containing activated carbon and no pH adjustment was done. The suspensions were placed on an orbital shaker and shaken at 200 rpm at room temperature for pre-determined period of time. At the end of time period, the suspension was filtered through a filter paper for separation of activated carbon from solution of residual AMX, filtrate. The filtrates was analyzed for residual AMX concentration using a UV–vis spectrometer (UV-160A, Shimadzu) at a wavelength of 196 nm.

The adsorbed amount of AMX per unit mass of activated carbon at any time t (Q_t) and the percentage of removal efficiency were calculated by equations 2 and 3 as follows (Liu et al., 2016):

$$Q_t = \frac{C_i - C_f}{m} \times V \quad (2)$$

$$Removal\ efficiency, \% = 100 \times \frac{C_i - C_f}{C_i} \quad (3)$$

where C_i ($mg.L^{-1}$) is initial concentration, C_f ($mg.L^{-1}$) is the concentration at the end of batch experiment, $V(L)$ is the volume of AMX solution and m (g) is the mass of activated carbon.

Kinetic data was obtained by batch experiments varying the time from 5 to 1440 min and analysed using pseudo-first order kinetic model, pseudo-second order kinetic

models and intra-particle diffusion model. The mathematical equations of pseudo-first order kinetic model, pseudo-second order kinetic model and intra-particle diffusion kinetic model are given in equations 4, 5, 6, respectively, as follows (Chayid and Ahmed, 2015):

$$\ln(Q_e - Q_t) = lnQ_e - k_1t \tag{4}$$

$$\frac{t}{Q_t} = \frac{1}{k_2 Q_e^2} - \frac{t}{Q_e} \tag{5}$$

$$Q_t = k_i t^{0.5} + C_i \tag{6}$$

Q_t and Q_e (mg.g^{-1}) are amount of AMX adsorbed at any time t (min) and at equilibrium time, respectively. k_1, k_2 and k_i are rate constants of first order, pseudo second order, and intra-particle diffusion kinetic model, respectively. C_i (mg.g^{-1}) is the boundary layer thickness.

Adsorption equilibrium experiments were carried out with AMX solutions at different initial concentrations (75-250 mg.L^{-1}) for an equilibrium time of 24 h in order to determine the AMX adsorption capacity of activated carbons in equilibrium state. At the end of experiments, AMX equilibrium concentration, C$_e$ and quantity of AMX adsorbed by 1 g activated carbon, Q$_e$ were determined. The relation between C$_e$ and Q$_e$ was established using Equations 7 and 8 specific to Freundlich and Langmuir adsorption isotherm models, respectively, given as follows (Moussavi et al., 2013):

$$\frac{C_e}{Q_e} = \frac{1}{K_L Q_{max}} + \frac{1}{Q_{max}} C_e \tag{7}$$

$$\log Q_e = \log K_F + \frac{1}{n} \log C_e \tag{8}$$

where Q_{max} is the maximum monolayer adsorption capacity, K_L is the equilibrium constant, K_F is the Freundlich constant, an empirical parameter related with the adsorption capacity, and *1/n* is the heterogeneity factor taking values usually in the range of 0-1. The *1/n* values closer to 0 indicates a more heterogeneous adsorbent surface (Edet and Ifelebuegu, 2020). In addition, separation factor (R$_L$), which is specific to Langmuir model, was calculated by equation 9 given below (Moussavi et al., 2013):

$$R_L = \frac{1}{1 + C_i K_L} \tag{9}$$

The value of R$_L$ helps to identify adsorption process as irreversible ($R_L = 0$), favorable ($0 < R_L < 1$), linear ($R_L = 1$), or unfavorable ($R_L > 1$) (Araújo et al., 2021).

3. Results and Discussion
3.1. Mass Yields and Carbon Recovery of Hydrochars
The mass yield and carbon recovery of hydrochars produced from legume wastes at different process temperature is given in Figure 1.
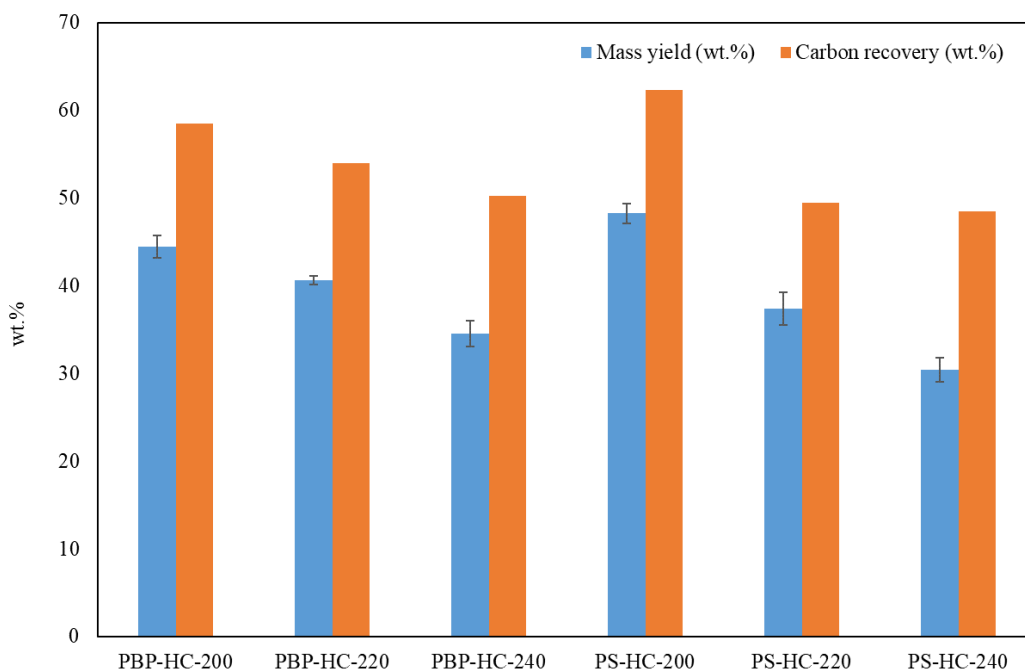
Figure 1. Mass yield and carbon recovery of hydrochars produced from dried legume wastes at different temperatures (dry basis) (wt.%).

As can be seen from Figure 1, a sharp decrease is observed in hydrochar yield with the increase of process temperature. It must be noted that PBP and PS have high holocellulose content which were reported as 79% (De Sa et al., 2022) and 61% (Verma et al., 2011) in the literature, respectively. Therefore, the sharp decrease of hydrochar yield with increasing process temperature was attributed to the enhanced degradation of legume wastes occuring

mainly as the hydrolysis of hemicellulose and cellulose in legume wastes (Kambo and Dutta, 2015; Makela et al., 2015). The carbon recovery of hydrochars was also shown in Figure 1. The weight percentage of carbon in legume waste recovered in hydrochar varied in the range of 48-57 wt% and 44-63 wt% in case of PBP and PS, respectively. These values were found to be lower than the carbon recovery results given in the literature (Kantarli, 2023;

Balmuk et al., 2023; Pala et al., 2014; Hoffmann et al., 2019) mainly due to the lower hydrochar yields obtained as a result of degradation of the higher holocellulose content of legume wastes in this study.

3.2. Fuel Properties of Hydrochars
Proximate, elemental, and energy analysis results of hydrochars derived from legume wastes at different process temperatures are given in Table 2.

Table 2. Proximate, elemental and energy analysis of hydrochars (dry basis)

	Proximate analysis, %wt., dry basis				Elemental analysis, %wt., dry basis					Energy analysis		
	Ash	VM	FC	FR	C	H	N	S	O	HHV [MJ/kg]	EDR	EY
PBP-HC-200	1.0	72.9	26.1	0.36	56.86	5.98	1.12	0.00	31.55	26.76	1.20	53.29
PBP-HC-220	1.1	67.9	30.9	0.45	58.26	5.68	1.10	0.00	29.56	26.89	1.20	48.97
PBP-HC-240	1.2	59.8	39.0	0.65	70.12	5.86	1.49	0.00	18.05	31.21	1.40	42.46
PS-HC-200	4.5	67.9	27.6	0.41	57.13	5.38	3.97	0.00	32.50	25.77	1.21	58.19
PS-HC-220	5.4	65.5	29.1	0.44	57.66	5.61	3.42	0.00	32.17	26.27	1.23	49.42
PS-HC-240	4.5	65.5	30.0	0.46	63.07	5.57	4.14	0.01	26.01	28.06	1.31	39.97

VM= volatile matter; FC= fixed carbon; FR (Fuel ratio)= FC / VM; HHV= higher heating value; EDR (energy densification ratio)= HHVhydrochar/ HHVbiomass; EY (energy yield) = mass yield × EDR; O% = 100 – (C+H+N+S+Ash).

The ash contents of PBP-derived hydrochars were lower than that of PBP owing to the solubility of inorganics under subcritical water conditions (Tables 1-2). Calculations depending on the hydrochar yield and ash contents revealed that 12-9 % of initial ash in PBP were retained in the resultant hydrochar depending on the process temperature. On the contrary to PBP-derived hydrochars, PS-derived hydrochars had ash contents only slightly lower/higher than that of PS due to the less solubility of inorganics under subcritical water conditions. Therefore, percentage of initial ash retained in PS-derived hydrochars were calculated to be in the range of 43-27% which were much higher than that retained in PBP-derived hydrochars. As can be seen from Table 2, HTC decreased the VM content of legume wastes, while it increased the FC content of legume wastes. This indicated the improvement of the carbon stability by HTC treatment. In case of PS, VM content of obtained hydrochar decreased only slightly (from 67.9% to 65.5%) and its FC content increased slightly (from 27.6% to 30.0%) with increasing temperature from 200 ºC to 240 ºC. Hence, HTC of PS led to the limited increase of FR of raw waste only from 0.23 to 0.44 which was still lower than 0.6 reported for lignite coal (Odeh, 2015). Compared to PS, VM content of PBP-derived hydrochar decreased pronouncedly from 72.9% to 59.8%, while its FC content increased pronouncedly from 26.1% to 39.0% with increasing temperature from 200ºC to 240ºC. HTC of PBP led to a higher increase of FR of raw biomass from 0.23 to 0.65 which is even higher than 0.6 reported for lignite coal (Odeh, 2015). Hydrochars had higher carbon content and lower oxygen content than legume wastes as a result of HTC. The effect of HTC temperature on carbon content of hydrochar was

noticable at 240 °C. C content of PBP-derived hydrochar and PS-derived hydrochar increased to 70.1% and 63.1% with the increase of HTC temperature to 240 °C, respectively. C content of PS-HC-240 was found to be higher than those of hydrochars obtained from pea pods at 230 °C for a duration of 30-480 min (Dong et al., 2019). The variation of HHV and ED of hydrochars showed similarity with the variation of carbon content. HHV of PBP-HC-240 was found to be higher than that of PS-HC-240 due to its higher C content. Comparision of the results with those in literature revealed that HHV of PBP-HC-240 was comparable to HHVs of hydrochars obtained by HTC of two-phase olive mill waste at 240-260 °C for 1-4 h (Balmuk et al., 2023), walnut and hazelnut shells at 250 °C for 24 h. (Pavkov et al., 2022) and from food waste at 230-260 °C for 30 min. (McGaughy and Reza, 2018) and higher than HHVs of hydrochars obtained by HTC of hornbeam wood at 275 °C for 1 h (Ercan et al., 2023), pineapple peelings at 250-270 °C for 5h (Bote et al., 2023), loquat seeds at 150-250 °C for 2-6 h (Kalderis et al., 2023), sunflower stalks at 180-280 °C for 45 min. (Nawaz and Kumar, 2023), cannabis waste at 170-230 °C for 1 h (Kanchanatip et al., 2022) and agricultural wastes at 180-260 °C for 1 h. (Wu et al., 2023). EY of PBP-derived hydrochars and PS-derived hydrochars decreased from 53.3% to 42.5% and from 58.2 % to 40.0 % with increasing temperature. The decreasing trend of EY with the increase of temperature, which was consistent with the literature (Kanchanatip et al., 2022; Kalderis et al., 2023), was mainly attributed to the dominance of reduction in mass yield over the increase of ED. EY values of hydrochars obtained in this study was similar to those observed by Kalderis et al. (2023) owing to the low mass

yield, while they were lower than those observed by Kanchanatip et al. (2022) owing to much higher mass yield obtained in their study. The atomic H/C ratio versus O/C ratio of hydrochars were plotted on the van Krevelen diagram, given in Figure 2, in order to follow the carbonization degree and identify the main reaction pathways during HTC.
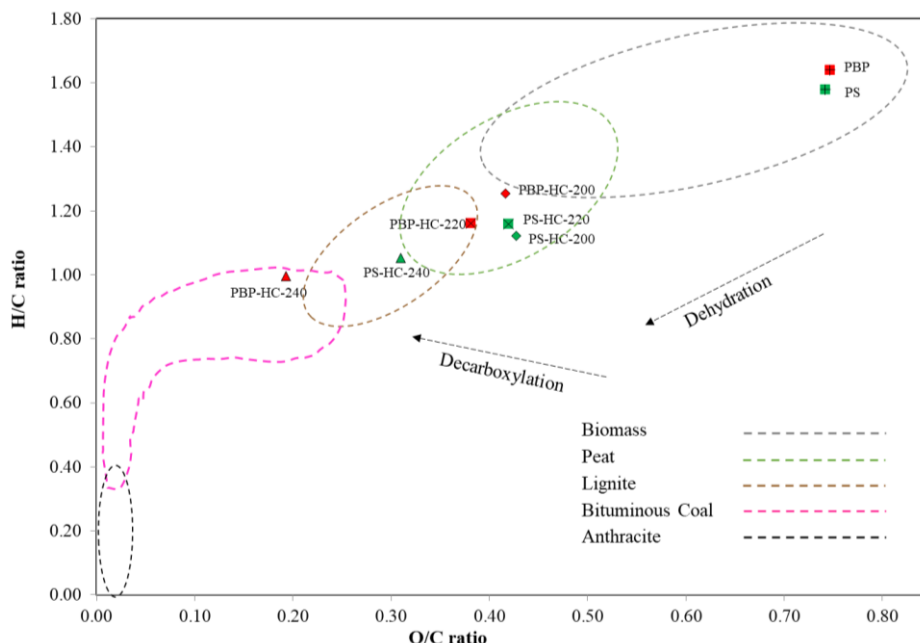
Figure 2. Van Krevelen diagram of hydrochars produced from legume wastes at different temperatures.

Examination of Figure 2 shows that dehydration reactions mainly occur at 200 °C, while decarboxylation reactions start to accompany dehydration reactions at 220 °C during HTC of PS. On the other hand, decarboxylation reactions accompany dehydration reactions at each temperature during HTC of PBP. Therefore, PBP-derived hydrochars had better carbonization degree than PS-derived hydrochars. As can be seen from Figure 2, PBP-HC-240 fall within the H/C and O/C ratio range of bituminous coal, while PS-HC-240 could only fall within the H/C and O/C ratio range of lignite. PS-HC-200 and PS-HC-220 fall in the region of peat which is consistent with the results obtained from HTC of pea pods at less severe conditions by Dong et al. (2019).

3.3 Activated Carbon Characteristics
PBP-HC-220 and PS-HC-220 were selected as activated carbon precursor in the $ZnCl_2$ activation experiments at 500 °C in order to obtain activated carbon with developed porosity at acceptable yield. Activated carbons obtained from PBP-derived and PS-derived hydrochars were abbreviated as PBP-AHC and PS-AHC, respectively.

3.3.1. Elemental composition and yields of activated carbons
Elemental analysis and mass yields of PBP-AHC and PS-AHC are presented in Table 3. Mass yield of activated carbon was calculated as the ratio of weight of activated carbon to weight of dried legume waste.

Table 3. Elemental analysis and mass yields of PBP-AHC and PS-AHC

	Elemental analysis, wt%				Yield, wt%
	C	H	N	O	
PBP-AHC	88.43	2.59	1.86	7.12	21.2
PS-AHC	82.02	2.91	4.63	10.44	22.6

The mass yields of PBP-AHC and PS-AHC were found as 21.2 and 22.6 %, respectively (Table 3). These mass yields were lower than those obtained by chemical activation of lignocellulosic waste-derived hydrochars given in the literature (Kantarli, 2023; Chen et al., 2017). Activation of hydrochars resulted in further increase of C contents accompanied by the decrease of H and O contents of resultant activated carbons which implied the enhancement of aromaticity in hydrochars.

3.3.2. BET surface area and pore volumes of activated carbons
BET surface area, mesopore volumes, and pore volumes of PBP-AHC and PS-AHC are given in Table 4. $ZnCl_2$ activation seems to be effective on the porosity development of legume waste-derived hydrochars (Table 4). As a result, both of the activated carbons had high surface area and total pore volume, which were comparable to or higher than those of activated carbons obtained by $ZnCl_2$ activation of wood sawdust hydrochar (Nirmaladevi and

Palanisamy, 2021), brewed tea waste hydrochar (Kantarli, 2023); KOH activation of garlic peel hydrochars (Huang et al., 2019) and raw coffee husk hydrochar (Tran et al, 2021) and K_2CO_3 activation of rice straw hydrochar (Liu et

al., 2014). PBP-AHC was found to have a higher BET surface area and more developed porosity than PS-AHC. This result was consistent with the higher C content observed for PBP-AHC (Table 3).

Table 4. BET surface area, mesopore volume, and pore volumes of PBP-AHC and PS-AHC

	BET Surface area ($m^2.g^{-1}$)	Mesopore area ($m^2.g^{-1}$)	Total pore volume ($cm^3.g^{-1}$)	Mesopore volume ($cm^3.g^{-1}$)
PBP-AHC	1350	399	0.723	0.249
PS-AHC	1205	152	0.686	0.144

3.4. FTIR Analysis of Legume Wastes, Hydrochars and Activated Carbons

FTIR analysis of legume wastes, their hydrochars obtained at 200°C and activated carbons was performed in order to detect the changes of chemical structure during HTC of legume wastes and chemical activation of hydrochars, respectively. FTIR spectra of legume wastes, their hydrochars, and activated carbon are given in Figure 3.
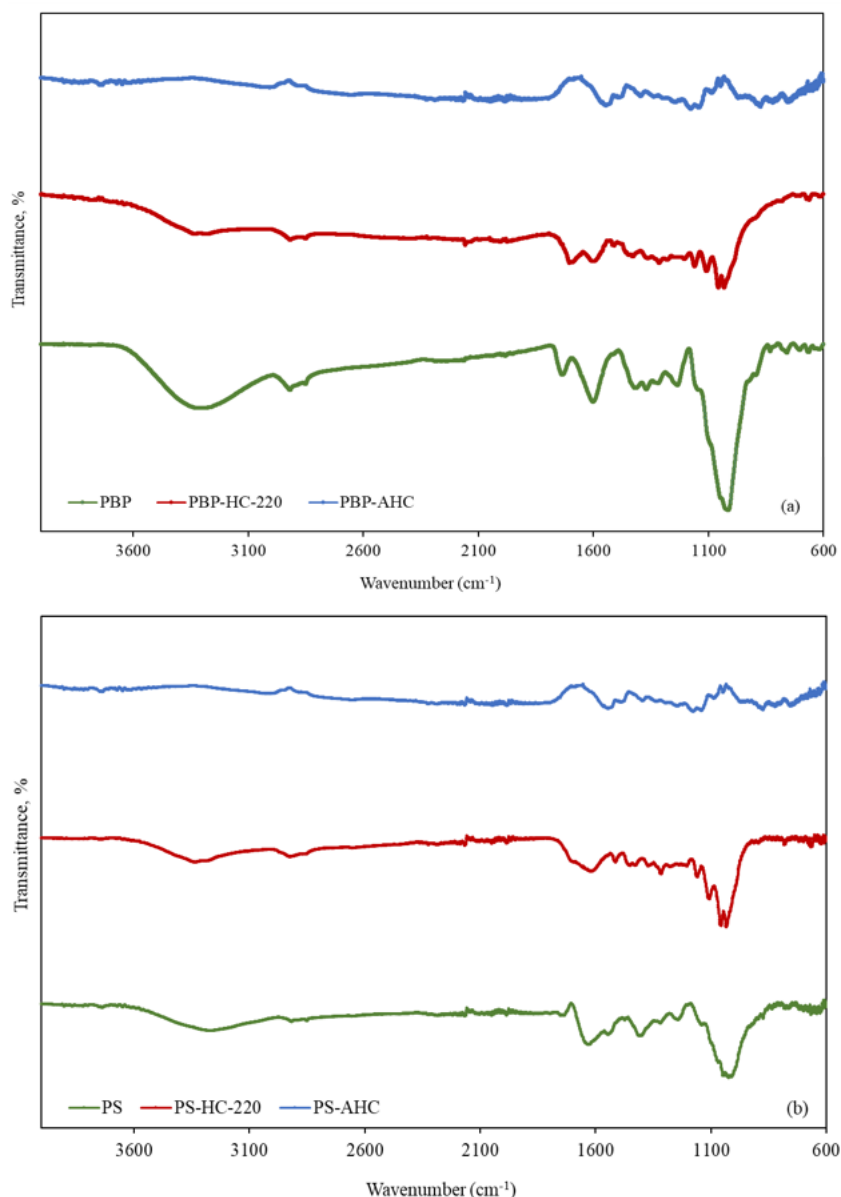
Figure 3. FTIR spectra of (a)PBP, PBP-HC-200, and PBP-AHC; (b)PS, PS-HC-200, and PS-AHC.

A wide peak was noticed in the spectra of PBP, PS, and all hydrochars at 3160-3600 cm⁻¹. This peak was attributed to the O-H stretching of the hydroxyl or carboxyl group. It must be noted that this peak was weaker in the spectra of

hydrochars as a result of dehydration during HTC and almost disappeared after $ZnCl_2$ activation. The peak at 2925-2850 cm⁻¹ was more strongly observed in the spectra of PBP and its hydrochar and attributed to the

aliphatic C-H stretching vibration of methylene groups of lignin (Missaoui et al., 2017). The existence of this peak in the spectra of both hydrochars implied that lignin was not completely decomposed during HTC. After activation, this peak was observed to be very weak which implied that further degradation of lignin occured during activation. The intensity of the peak around 1030 cm^{-1} corresponding to the C-O stretching of hemicellulose and cellulose (Missaoui et al., 2017) weakened as a result of their partial degradation during HTC. This peak almost disappeared after ZnCl$_2$ activation showing that degradation of holocellulose in legume wastes was almost completed.

The peak at 1740 cm^{-1} existing in the spectra of legume wastes corresponds to the C=O stretching of ester group of hemicellulose. This peak disappeared due to the degradation of hemicellulose after HTC (Dong et al., 2019)

and a new peak appeared at 1690 cm^{-1} implying the formation of carbonyl/carboxyl groups conjugated to a benzene ring or C=C bond. The peak which was observed at 1635 cm^{-1} in the spectrum of legume wastes and shifted to 1610 cm^{-1} in the spectra of hydrochars was assigned to C=C aromatic stretching (Wang et al., 2018; Dong et al., 2019). The C=O peaks disappeared and C=C peaks shifted to lower wavenumbers after ZnCl$_2$ activation of both type of hydrochars implying the enhancement of decarboxylation and improvement of aromaticity.

3.5. SEM Analysis of Legume Wastes, Hydrochars and Activated Carbons

The SEM images of legume wastes, their hydrochars, and activated carbons taken at × 2500 magnitude are given in Figure 4.
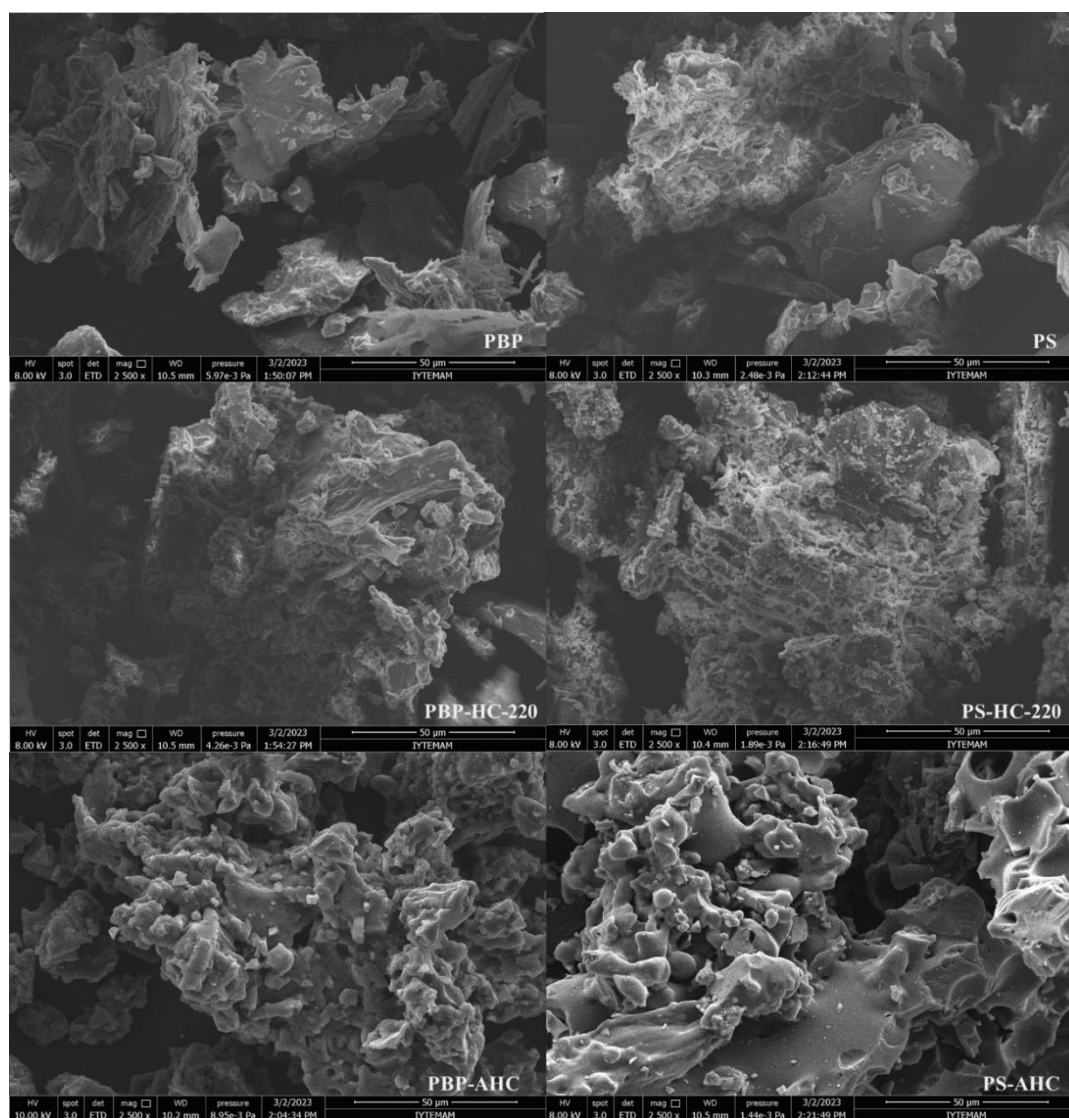
Figure 4. SEM images of legume wastes, their hydrochars, and activated carbons (×2500 magnitude).

The changes in morphologies of legume wastes after HTC and ZnCl$_2$ activation can be followed from SEM images given in Figure 4. The surface of legume wastes was smooth. On the other hand, the surface of hydrochars was observed to be relatively rough and deformed compared

to that of legume wastes which was attributed to the degradation of hemicellulose and cellulose into smaller fragments during HTC (Hamid and Subramaniam, 2022). According to Chen et al. (2017), these smaller fragments might combine to form spherical particles on the surface

of hydrochars during HTC. Similarly, a number of spherical particles was detected on the surface of hydrochars in this study. Also, a small number of rudimentary pores was observed on the surface of hydrochars which might have occured through removal of internal volatile fraction in legume wastes. Further treatment of hydrochars by $ZnCl_2$ activation resulted in more porous morphology as can be seen from SEM images of activated carbons given in Figure 4. Spherical particles seems to retain on the surface even after activation of hydrochars.

3.6. AMX Adsorption Study

3.6.1. Effect of time on AMX removal efficiency and adsorption kinetics

Batch adsorption experiments were carried out for PBP-AHC and PS-AHC at adsorption times varying between 1 and 24 h with an amount of 0.075 g (3 g.L^{-1}) in a 25 mL of 200 ppm AMX solution in order to determine the equilibrium time. Variation of removal efficiency with time was presented in Table 5. PBP-AHC showed higher removal efficiency in shorter adsorption time probably due to its higher surface area which probably enabled a faster mass transfer (Table 5). Therefore, AMX removal efficiency of PBP-AHC changed very slightly with the increase of adsorption time. None of the activated carbons was able to achieve a removal efficiency of 100% even for an adsorption time of 24 h which was attributed to the high initial concentration of AMX. 24 h was chosen as the equilibrium time in order to guarantee the establishment of adsorption equilibrium for both activated carbons.

Table 5. Removal efficiency of activated carbon at different adsorption times, %

		Adsorption time, hour				
		1	2	4	6	24
Removal efficiency (%)	PBP-AHC	86.9	87.4	87.9	88.2	89.7
	PS-AHC	77.2	81.8	83.1	84.1	87.3

Adsorption kinetic study was carried out at an initial AMX concentration of 200 ppm varying the time between 10 and 1440 minutes. Q_t versus time was plotted using the data obtained and was shown in Figure 5. As can be seen from the figure, AMX adsorption rate was fast at the initial stage of adsorption and got slower with the increase of time.
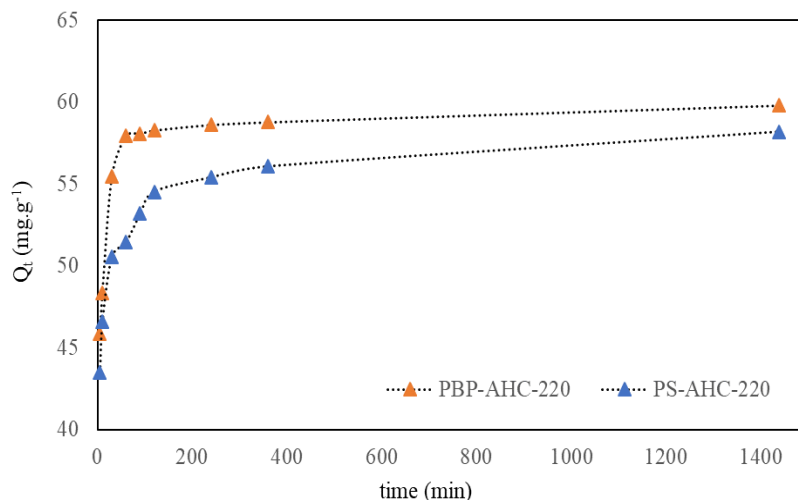
Figure 5. Plot of adsorbed amount of AMX per unit mass of activated carbon (Q_t) versus time.

Kinetic parameters of AMX adsorption on PBP-AHC and PS-AHC obtained from the analysis of kinetic data using pseudo-first order kinetic model, pseudo-second order kinetic model and intra-particle diffusion kinetic model were presented in Table 6.

The comparison of R^2 values in Table 6 revealed that AMX adsorption on PBP-AHC and PS-AHC best fits with the pseudo-second order kinetic model and hence AMX adsorption rate is controlled mainly by chemisorption. $Q_{e,2}$ values calculated from pseudo-second order model were found to be more proximate to $Q_{e,experimental}$ values than Q_e values calculated from other models. Comparison of k_2 values showed that AMX adsorption rate of PBP-AHC was

faster than that of PS-AHC. The compatibility of pseudo-second order kinetic model for AMX adsorption on activated carbon was also reported by other researchers in the literature (Chayid and Ahmed, 2015; Budyanto et al., 2008; Moussavi et al., 2013).

3.6.2. Effect of activated carbon dosage on AMX removal efficiency

Effect of activated carbon dosage on AMX removal efficiency of both activated carbon was investigated and depicted in Figure 6. As can be seen from Figure 6, removal efficiency of AMX increased proportionally (from 30.0% and 28.8% to 82.8% and 83.0% for PBP-AHC and PS-AHC, respectively) with increasing activated carbon dosage

from 0.5 to 2 g.L^{-1}. Further increase of activated carbon dosage caused only a slight increase in removal efficiency of AMX without achieving 100% removal.

3.6.3. Adsorption isotherms

Adsorption isotherm study was performed at an activated carbon dosage of 3 g. L^{-1} at varying initial AMX concentrations (75 - 250 ppm) for an equilibrium time of 24 h. Activated carbon dosage was selected as 3 g. L^{-1}, since maximum AMX removal efficiency was achieved at this dosage (Figure 6). Isotherm constants and R^2 values of Langmuir and Freundlich models obtained by application of Equations 7 and 8 to the C_e and Q_e values determined at different initial concentrations are given in Table 7.
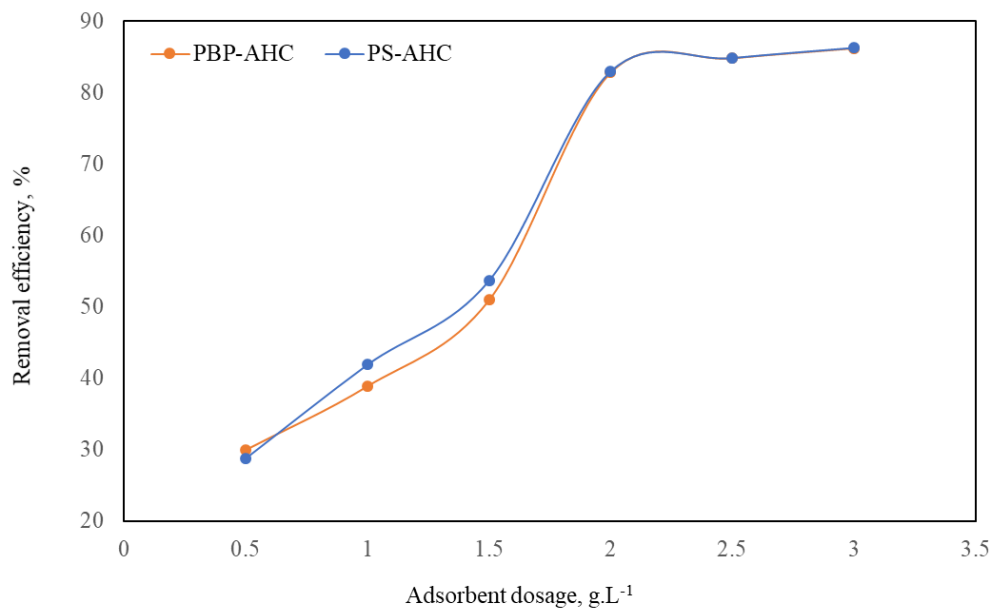
Figure 6. Effect of activated carbon dosage on removal efficiency of AMX.

Table 6. Kinetic parameters of AMX adsorption on PBP-AHC and PS-AHC.

	PBP-AHC	PS-AHC
$Q_{e,exp}$	59.79	58.18
Pseudo-first order model		
k_1	0.0103	0.0049
Q_{e1} (mg.g^{-1})	7.79	10.25
R^2	0.664	0.883
Pseudo-second order model		
k_2	0.0084	0.0048
Q_{e2} (mg.g^{-1})	59.17	56.49
R^2	0.999	0.999
Intra-particle diffusion model		
C_{i1}(mg.g^{-1})	39.32	41.46
C_{i2}(mg.g^{-1})	57.24	51.05
k_{i1}	2.81	1.41
k_{i2}	0.09	0.27
R^2_1	0.962	0.892
R^2_2	0.987	0.895

$Q_{e,exp}$ (mg.g^{-1})= amount of AMX adsorbed at equilibrium obtained in experiments, k_1= pseudo-first order, model rate constant,Q_{e1} (mg.g^{-1})= amount of AMX adsorbed at equilibrium time calculated by pseudo-first, order model, k_2= pseudo-second order model rate constant, Q_{e2} (mg.g^{-1})= amount of AMX adsorbed, at equilibrium time calculated by pseudo-second order model, k_{i1}= intra-particle diffusion model first, stage rate constant, k_{i2}= intra-particle diffusion model second stage rate constant, C_{i1} (mg.g^{-1})= the first, stage boundary layer thickness, C_{i2} (mg.g^{-1})= the second stage boundary layer thickness.

Table 7. Langmuir and Freundlich isotherm constants and R^2 values for AMX adsorption on PBP-AHC and PS-AHC

	PBP-AHC	PS-AHC
Langmuir		
Q_{max} (mg.g^{-1})	188.7	70.9
K_L (L.mg^{-1})	0.02	0.23
R_L	0.155	0.017
R^2	0.96	0.98
Freundlich		
$1/n$ (mg.g^{-1})	0.73	0.29
K_F (L.mg^{-1})	6.26	22.85
R^2	0.99	0.95

Q_{max}= maximum monolayer adsorption capacity, K_L= equilibrium constant, R_L: separation factor, K_F= Freundlich constant, $1/n$= heterogeneity factor.

R^2 values of Langmuir and Freundlich isotherms presented in Table 7 indicated that experimental isotherm data of PBP-AHC and PS-AHC were highly correlated with both of the models. In case of AMX adsorption on PS-AHC, Freundlich isotherm showed more satisfactory fit with the experimental data. This indicated that adsorption took place on the surface of PS-AHC which was energetically heterogeneous. On the other hand, Langmuir isotherm was found to be more compatible with the experimental data of PBP-AHC indicating that AMX molecules covered the surface of PBP-AHC, which was homogeneous, as monolayer.

Examination of Langmuir isotherm constants revealed that AMX adsorption onto PBP-AHC was favorable ($0 < R_L < 1$), while that on PS-AHC was nearly irreversible ($R_L \approx 0$) (Araújo et al., 2021). Similarly, 1/n values calculated from Freundlich isotherm model also indicated a favorable AMX adsorption on both activated carbons (Kalam et al., 2021).

Q_{max} values are known to be very useful for determination and comparison of adsorption capacities of adsorbents. As can be seen from Table 7, PBP-AHC has much higher AMX adsorption capacity than PS-AHC due to its more developed porosity with more mesoporous character and higher surface area. Rodrigues et al. stated that predominantly mesoporous activated carbons having oxygenated groups in abundance and high specific area shows an efficient and fast AMX adsorption (Rodrigues et al., 2020). Hence, it can be stated that PBP derived hydrochar is a more promising precursor in production of activated carbon with a good AMX adsorption capacity. Q_{max} of AMX on other activated carbons was calculated as 345 mg. g^{-1} for KOH activated giant reed (Chayid and Ahmed, 2015); 233 mg.g^{-1} for coconut shell based commercial activated carbon (Budyanto et al., 2008); 439 mg.g^{-1} for NH$_4$Cl activated pomegranate wood (Moussavi et al., 2013); 175 and 268 mg.g^{-1} for two types of magnetic activated carbon (Saucier et al., 2017); 122 and 132 mg.g^{-1} for Mn-impregnated *Phragmites australis* based activated carbons (Liu et al., 2016) and 130 and 176 mg.g^{-1} for two types of ZnCl$_2$ activated solid olive-mill waste (Rodrigues et al., 2020) in literature. Depending on the literature results, KOH or NH$_4$Cl activation of PBP-HC-220 and PS-HC-220 can be investigated in further studies to obtain a higher AMX adsorption capacity.

4. Conclusion

In this study, use of hydrochars obtained from legume wastes as fuel and their conversion into activated carbon for amoxicillin removal was investigated. Two types of legume wastes, pinto bean peels and pea shells, were used for hydrochar production. Hydrothermal carbonization of legume wastes was carried out at different temperatures in order to examine its effect on fuel properties of derived hydrochars. Hydrothermal carbonization at 240 ∘C had significant effect on the enhancement of hydrochar fuel properties such as higher heating value and fuel ratio. This effect was more noticeable in case of pinto bean shells. Van Krevelen Diagram depicted the formation of bituminous coal-like and lignite-like hydrochars from pinto bean peels and pea shells at 240 ∘C, respectively. Initial ash in pinto bean peels retained in the resultant hydrochar was lower than that in pea shell retained in the resultant hydrochar. This was attributed to the difference in ash composition of legume wastes. ZnCl$_2$ activation of hydrochars obtained at 220 °C produced activated carbons with enhanced surface area and pore volume that varied according to the legume waste type. Pinto bean peel yielded an activated carbon with higher BET surface area, total pore volume, mesopore volume and hence maximum amoxicilline adsorption capacity and rate. Overall, it can be concluded that hydrothermal carbonization can be considered as a promising treatment method of legume wastes for enhancing their fuel properties and as a promising pretreatment method of legume wastes for activated carbon production by chemical activation.

Author Contributions

Percentages of the author contributions is present below. The author reviewed and approved final version of the manuscript.

	İ.C.K.
C	100
D	100
S	100
DCP	100
DAI	100
L	100
W	100
CR	100
SR	100

C= concept, D= design, S= supervision, DCP= data collection and/or processing, DAI= data analysis and/or interpretation, L= literature search, W= writing, CR= critical review, SR= submission and revision.

Conflict of Interest

The author declared that there is no conflict of interest.

Ethical Consideration

Ethics committee approval was not required for this study because of there was no study on animals or humans.

References

Abazari R, Mahjoub AR. 2018. Ultrasound-assisted synthesis of Zinc(II)-based metal organic framework nanoparticles in the presence of modulator for adsorption enhancement of 2,4-dichlorophenol and amoxicillin. Ultrason Sonochem, 42: 577-584. DOI: 10.1016/j.ultsonch.2017.12.027.

Ajala OO, Akinnawo SO, Bamisaye A, Adedipe DT, Adesina MO, Okon-Akan OA, Adebusuyi TA, Ojedokun AT, Adegoke KA, Bello OS. 2023. Adsorptive removal of antibiotic pollutants from wastewater using biomass/biochar-based adsorbents. RSC Adv, 13: 4678-4712 DOI:10.1039/d2ra06436g.

Akogun OA, Waheed MA. 2019. Property upgrades of some raw Nigerian biomass through torrefaction pre-treatment- a review. J Phys, 1378: 032026. DOI:10.1088/1742-6596/1378/3/032026.

Angın D, Köse TE, Selengil U. 2013a. Production and characterization of activated carbon prepared from safflower seed cake biochar and its ability to absorb reactive dyestuff. Appl Surf Sci, 280: 705-710. DOI: 10.1016/j.apsusc.2013.05.046.

Angın D, Altintig E, Köse TE. 2013b. Influence of process parameters on the surface and chemical properties of activated carbon obtained from biochar by chemical activation. Bioresour Technol, 148: 542-549. DOI: 10.1016/j.biortech.2013.08.164.

Araújo LK, Albuquerque AA, Ramos WC, Santos AT, Carvalho SH, Soletti JI, Bispo MD. 2021. Elaeis guineensis-activated carbon for methylene blue removal: adsorption capacity and optimization using CCD-RSM, Environ Dev Sustain 1-19. DOI: 10.1016/j.crgsc.2022.100325.

Balarak D, Mahdavi Y, Maleki A, Daraei H, Sadeghi S. 2016. Studies on the removal of amoxicillin by single walled carbon nanotubes. Br J Pharmaceut Res, 10(4): 1-9. DOI: 10.9734/BJPR/2016/24150.

Balmuk G, Cay H, Duman G, Kantarli IC, Yanik J. 2023. Hydrothermal carbonization of olive oil industry waste into solid fuel: Fuel characteristics and combustion performance. Energy, 278:127803. DOI: 10.1016/j.energy.2023.127803.

Bote JG, Castasus NFP, Layug KM, Vicente RZ, Yambao PJT, Rubi RVC, Roque EC, Olay JG. 2023. Production of hydrochar using pineapple (Ananas comosus) peelings via hydrothermal carbonization, Mater Today-Proc. Article in press. DOI:10.1016/j.matpr.2023.05.464.

Budyanto S, Soedjono S, Irawaty W, Indraswati N. 2008. Studies of adsorption equilibria and kinetics of amoxicillin from simulated wastewater using activated carbon and natural bentonite. J Environ Prot Sci, 2: 72-80.

Channiwala SA, Parikh PP. 2002. A unified correlation for estimating HHV of solid, liquid and gaseous fuels. Fuel, 81(8): 1051-1063. DOI: 10.1016/S0016-2361(01)00131-4.

Chayid M, Ahmed MJ. 2015. Amoxicillin adsorption on microwave prepared activated carbon from Arundo donax Linn: Isotherms, kinetics, and thermodynamics studies. J Environ Chem Eng, 3: 1592-1601. DOI: 10.1016/j.jece.2015.05.021.

Chen J, Zhang L, Yang G, Wang Q, Li R, Lucia LA. 2017. Preparation and characterization of activated carbon from hydrochar by phosphoric acid activation and its adsorption performance in prehydrolysis liquor. BioRes, 12(3): 5928-5941. DOI: 10.15376/biores.12.3.5928-5941.

Ciolkosz D, Wallace R. 2011. A review of torrefaction for bioenergy feedstock production. Biofuel Bioprod Bior, 5(3): 317-329. DOI: 10.1002/bbb.275.

De Franco MAE, de Carvalho CB, Bonetto MM, de Pelegrini Soares R, Feris LA. 2017. Removal of amoxicillin from water by adsorption onto activated carbon in batch process and fixed bed column: Kinetics, isotherms, experimental design and breakthrough curves modelling. J Clean Prod, 161: 947-956. DOI: 10.1016/j.jclepro.2017.05.197.

De Sa IC, De Oliveira P, Nossol E, Borges PHS, Lepri FG, Semaan FS, Pacheco WF. 2022. Modified dry bean pod waste (Phaseolus vulgaris) as a biosorbent for fluorescein removal from aqueous media: batch and fixed bed studies. J Hazard Mater, 424: 127723. DOI: 10.1016/j.jhazmat.2021.127723.

Dong X, Guo S, Wang H, Wang Z, Gao X. 2019. Physicochemical characteristics and FTIR-derived structural parameters of hydrochar produced by hydrothermal carbonisation of pea pod (Pisum sativum Linn.) waste. Biomass Conv Bioref, 9: 531-540. DOI: 10.1007/s13399-018-0363-1.

Edet UA, Ifelebuegu AO. 2020. Kinetics, isotherms, and thermodynamic modeling of the adsorption of phosphates from model wastewater using recycled brick waste. Processes, 8(6): 665. DOI: 10.3390/pr8060665.

Elaigwu, SE, Rocher V, Kyriakou G, Greenway GM. 2014. Removal of Pb2+ and Cd2+ from aqueous solution using chars from pyrolysis and microwave-assisted hydrothermal

carbonization of Prosopis Africana Shell. J Ind Eng Chem, 20: 3467-73. DOI: doi.org/10.1016/j.micromeso.2012.08.006.

Elmolla ES, Chaudhuri M. 2010. Degradation of amoxicillin, ampicillin and cloxacillin antibiotics in aqueous solution by the UV/ZnO photocatalytic process. J Hazard Mater, 173: 445-449. DOI: 10.1016/j.jhazmat.2009.08.104.

Eom H, Kim J, Nam I, Bae S. 2021. Recycling black tea waste biomass as activated porous carbon for long life cycle supercapacitor electrodes. Materials, 14(21): Article 6592. DOI: 10.3390/ma14216592.

Ercan B, Alper K, Ucar S, Karagoz S. 2023. Comparative studies of hydrochars and biochars produced from lignocellulosic biomass via hydrothermal carbonization, torrefaction and pyrolysis. Journal of the Energy Institute,109:101298. DOI: 10.1016/j.joei.2023.101298.

Fazelirad H, Ranjbar M, Taher MA, Sargazi G. 2015. Preparation of magnetic multi-walled carbon nanotubes for an efficient adsorption and spectrophotometric determination of amoxicillin. J Ind Eng Chem, 21: 889-892. DOI: 10.1016/j.jiec.2014.04.028.

Fernandez ME, Ledesma B, Roman S, Bonelli PR, Cukierman AL. 2015. Development and characterization of activated hydrochars from orange peels as potential adsorbents for emerging organic contaminants. Bioresour Technol,183: 221-228. DOI: 10.1016/j.biortech.2015.02.035.

Flora JFR, Lu X, Li L, Flora JRV, Berge ND. 2013. The effects of alkalinity and acidity of process water and hydrochar washing on the adsorption of atrazine on hydrothermally produced hydrochar. Chemosphere, 93: 1989-96. DOI: 10.1016/j.chemosphere.2013.07.018.

Funke A, Reebs F, Kruse A. 2013. Experimental comparison of hydrothermal and vapothermal carbonization. Fuel Process Technol, 115: 261-269. DOI: 10.1016/j.fuproc.2013.04.020.

Garoma T, Umamaheshwar SH, Mumper A. 2010. Removal of sulfadiazine, sulfamethizole, sulfamethoxazole, and sulfathiazole from aqueous solution by ozonation. Chemosphere, 79: 814-20. DOI: 10.1016/j.chemosphere.2010.02.060.

Goswami R, Shim J, Deka S, Kumari D, Kataki R, Kumar M. 2016. Characterization of cadmium removal from aqueous solution by biochar produced from Ipomoea fistulosa at different pyrolytic temperatures. Ecol Eng, 97: 444-451. DOI: 10.1016/j.ecoleng.2016.10.007.

Hadjittofi L, Prodromou M, Pashalidis I. 2014. Activated biochar derived from cactus fibres – Preparation, characterization and application on Cu(II) removal from aqueous solutions. Bioresour Technol, 159: 460-464. DOI: 10.1016/j.biortech.2014.03.073.

Hamid SBA, Chowdhury ZZ, Zain SM. 2014. Base catalytic approach: A promising technique for the activation of biochar for equilibrium sorption studies of copper, Cu (II) ions in single solute system. Materials, 7 (4): 2815-2832. DOI: 10.3390/ma7042815.

Hamid NA, Subramaniam T. 2022. Physicochemical properties of hydrochars produced from Khaya senegalensis leaves using hydrothermal carbonisation. Journal of Engineering Science and Technology, 17(3): 1781-91.

Hayati B, Maleki A, Najafi F, Gharibi F, McKay G, Gupta VK, Puttaiah SH, Marzban N. 2018. Heavy metal adsorption using PAMAM/CNT nanocomposite from aqueous solution in batch and continuous fixed bed systems. Chem Eng J, 346: 258-270. DOI: 10.1016/j.cej.2018.03.172.

Heilmann SM, Davis HT, Jader LR, Lefebvre PA, Sadowsky MJ, Schendel FJ, Von Keitz MG, Valentas KJ. 2010. Hydrothermal carbonization of microalgae. Biomass Bioenergy, 34: 875-882.

DOI: 10.1016/j.biombioe.2010.01.032.

Heilmann, SM, Jader LR, Sadowsky MJ, Schendel FJ, Von Keitz MG, Valentas KJ. 2011. Hydrothermal carbonization of distiller's grains. Biomass Bioenergy, 35: 2526-2533. DOI: 10.1016/j.biombioe.2011.02.022

Hoffmann V, Jung D, Zimmermann J, Rodriquez Correa C, Elleuch A. 2019. Conductive carbon materials from the hydrothermal carbonization of vineyard residues for the application in electrochemical double-layer capacitors (EDLCs) and direct carbon fuel cells (DCFCs). Materials, 12(10): 1-33. DOI: 10.3390/ma12101703.

Horikawa T, Kitakaze Y, Sekida T, Hayashi J, Katoh M. 2010. Characteristics and humidity control capacity of activated carbon from bamboo. Bioresour Technol, 101: 3964-3969. DOI: 10.1016/j.biortech.2010.01.032

Huang GG, Liu YF, Wu XX, Cai JJ. 2019. Activated carbons prepared by the KOH activation of a hydrochar from garlic peel and their CO_2 adsorption performance. New Carbon Mater, 34(3): 247-257. DOI: 10.1016/S1872-5805(19)60014-4

Huff MD, Lee JW. 2016. Biochar-surface oxygenation with hydrogen peroxide. J Environ Manage, 165: 17-21. DOI: 10.1016/j.jenvman.2015.08.046.

Iriarte-Velasco U, Sierra I, Zudaire L, Ayastuy JL. 2016. Preparation of a porous biochar from the acid activation of pork bones. Food Bioprod Process, 98: 341-353. DOI: 10.1016/j.fbp.2016.03.003.

Islam MA, Benhouria A, Asif M, Hameed BH. 2015. Methylene blue adsorption on factory- rejected tea activated carbon prepared by conjunction of hydrothermal carbonization and sodium hydroxide activation processes. J Taiwan Inst Chem Eng, 52: 57-64. DOI: doi.org/10.1016/j.jtice.2015.02.010.

Islam MA, Ahmed MJ, Khanday WA, Asif M, Hameed BH. 2017. Mesoporous activated coconut shell-derived hydrochar prepared via hydrothermal carbonization-NaOH activation for methylene blue adsorption. J Environ Manage, 203: 237-244. DOI: 10.1016/j.jenvman.2017.07.029.

Jain A, Jayaraman S, Balasubramanian R, Srinivasan MP. 2014. Hydrothermal pre-treatment for mesoporous carbon synthesis: enhancement of chemical activation. J Mater Chem A, 2: 520-528. DOI: 10.1039/C3TA12648J.

Kalam S, Abu-Khamsin SA, Kamal MS, Patil S. 2021. Surfactant adsorption isotherms: a review. ACS Omega, 6 (48): 32342-348. DOI: 10.1021/acsomega.1c04661.

Kalderis D, Görmez Ö, Saçlı B, Çalhan SD, Gözmen B. 2023. Valorization of loquat seeds by hydrothermal carbonization for the production of hydrochars and aqueous phases as added-value products. J Environ Manage, 344: 118612. DOI: 10.1016/j.jenvman.2023.118612.

Kambo HS, Dutta A. 2015. Comparative evaluation of torrefaction and hydrothermal carbonization of lignocellulosic biomass for the production of solid biofuel. Energy Convers Manage, 105: 746-755. DOI: /10.1016/j.enconman.2015.08.031.

Kanchanatip E, Prasertsung N, Thasnas N, Grisdanurak N, Wantala K. 2022. Valorization of cannabis waste via hydrothermal carbonization: solid fuel production and characterization. Environ Sci Pollut Res. DOI:10.1007/s11356-022-24123-0

Kantarli IC, Kabadayi A, Ucar S, Yanik, J. 2016. Conversion of poultry wastes into energy feedstocks. Waste Manage, 56: 530-539. DOI: 10.1016/j.wasman.2016.07.019.

Kantarli IC. 2023. Conversion of brewed tea waste into hydrochar and activated carbon. Int J Glob Warming, 29(1-2):1-15. DOI: 10.1504/IJGW.2023.128832.

Kerkez-Kuyumcu O, Bayazit SS, Salam MA. 2016. Antibiotic

amoxicillin removal from aqueous solution using magnetically modified graphene nanoplatelets. J Ind Eng Chem, 36:198-205. DOI: 10.1016/j.jiec.2016.01.040.

Laginhas C, Valente Nabais JM, Titirici MM. 2016. Activated carbons with high nitrogen content by a combination of hydrothermal carbonization with activation. Microporous and Mesoporous Mater, 226: 125-132. DOI: doi.org/10.1016/j.micromeso.2015.12.047.

Laksaci H, Belhamdi B, Khelif O, Khelif A, Trari M. 2023. Elimination of amoxicillin by adsorption on coffee waste based activated carbon. J Mol Struct, 1274: 134500.

Larsson SH, Rudolfsson M, Nordwaeger M, Olofsson I, Samuelsson R. 2013. Effect of moisture content, torrefaction temperature and die temperature in pilot scale pelletizing of torrefied Norway spruce. App Energy, 102: 827-832. DOI: 10.1016/j.apenergy.2012.08.046.

Limousy L, Ghouma I, Ouederni A, Jeguirim M. 2017. Amoxicillin removal from aqueous solution using activated carbon prepared by chemical activation of olive stone. Environ Sci Pollut Res, 24 (11): 9993-10004. DOI: 10.1007/s11356-016-7404-8.

Li H, Hu J, Cao Y, Li X, Wang X. 2017. Development and assessment of a functional activated fore-modified bio-hydrochar for amoxicillin removal. Bioresour Technol, 246:168-175. DOI: 10.1016/j.biortech.2017.06.112.

Lim WC, Srinivasakannan C, Balasubramanian N. 2010. Activation of palm shells by phosphoric acid impregnation for high yielding activated carbon. J Anal Appl Pyrolysis, 88: 181-186. DOI: 10.1016/j.jaap.2010.04.004

Liu Y, Zhu X, Qian F, Zhang S, Chen J. 2014. Magnetic activated carbon prepared from rice straw-derived hydrochar for triclosan removal. RSC Adv, 4(109): 63620-63626. DOI: 10.1039/c4ra11815d.

Liu H, Hu Z, Liu H, Xie H, Lu S, Wang Q, Zhang J. 2016. Adsorption of Amoxicillin by Mn-impregnated activated carbons: performance and mechanisms. RSC Adv, 6(14): 11454-11460. DOI: 10.1039/C5RA23256B.

Maitlo G, Ali I, Mangi KH, Ali S, Maitlo HA, Unar IN, Pirzada AM. 2022. Thermochemical conversion of biomass for syngas production: current status and future trends. Sustainability, 14(5):2596. DOI: 10.3390/su14052596.

Makela M, Benavente V, Fullana A. 2015. Hydrothermal carbonization of lignocellulosic biomass: effect of process conditions on hydrochar properties. Appl Energy,155:576-84. DOI: 10.1016/j.apenergy.2015.06.022.

Martínez-Castaño M, Mejía Díaz DP, Contreras-Calderón J, Gallardo Cabrera C. 2020. Physicochemical properties of bean pod (Phaseolus vulgaris) flour and its potential as a raw material for the food industry. Revista Facultad Nacional de Agronomía Medellín, 73(2): 9179-9187. DOI: 10.15446/rfnam.v73n2.81564.

Mateos-Aparicio I, Redondo-Cuenca A, Villanueva-Suárez MJ, Zapata-Revilla MA, Tenorio-Sanz, MD. 2010. Pea pod, broad bean pod and okara, potential sources of functional compounds. LWT- Food Sci Technol, 43:1467-1470. DOI: 10.1016/j.lwt.2010.05.008.

McGaughy K, Toufiq Reza M. 2018. Hydrothermal carbonization of food waste: simplified process simulation model based on experimental results. Biomass Conv Bioref, 8: 283-292. DOI: 10.1007/s13399-017-0276-4.

Missaoui A, Bostyn S, Belandria V, Cagnon B, Sarh B, Gokalp I. 2017. Hydrothermal carbonization of dried olive pomace: energy potential and process performances. J Anal Appl Pyrolysis,128: 281-90. DOI: 10.1016/j.jaap.2017.09.022.

Moradi SE. 2015. Highly efficient removal of amoxicillin from water by magnetic graphene oxide adsorbent. Chem Bull 'Politehnica'University Timisoara, Rom Ser Chem Environ Eng, 60: 41-48.

Moussavi G, Alahabadi A, Yaghmaeian K, Eskandari M. 2013. Preparation, characterization and adsorption potential of the NH4Cl-induced activated carbon for the removal of amoxicillin antibiotic from water. Chem Eng J, 217: 119-128. DOI:10.1016/j.cej.2012.11.069.

Nawaz A, Kumar P. 2023. Impact of temperature severity on hydrothermal carbonization:fuel properties, kinetic and thermodynamic parameters. Fuel, 336:127166. DOI: 10.1016/j.fuel.2022.127166.

Nirmaladevi S, Palanisamy PN. 2021. Adsorptive behavior of biochar and zinc chloride activated hydrochar prepared from Acacia leucophloea wood sawdust: kinetic equilibrium and thermodynamic studies. Desalination Water Treat, 209: 170-181. DOI: 10.5004/dwt.2021.26515

Odeh AO. 2015. Comprehensive conventional analysis of southern hemisphere coal chars of different ranks for fixed bed gasification. Global Journals of Research in Engineering, 15(4): 5-16.

Pala M, Kantarli IC, Buyukisik HB, Yanik J. 2014. Hydrothermal carbonization and torrefaction of grape pomace: A comparative evaluation. Bioresour Technol, 161: 255-262. DOI: 10.1016/j.biortech.2014.03.052.

Pari G, Darmawan S, Bambang Prihandoko B. 2014. Porous carbon spheres from hydrothermal carbonization and koh activation on cassava and tapioca flour raw material. Procedia Environmental Sciences, 20: 342-51. DOI: 10.1016/j.proenv.2014.03.043.

Parshetti GK, Chowdhury S, Balasubramanian R. 2014. Hydrothermal conversion of urban food waste to chars for removal of textile dyes from contaminated waters. Bioresour Technol, 161: 310-319. DOI: 10.1016/j.biortech.2014.03.087.

Pavkov I, Radojčin M, Stamenković Z, Bikić S, Tomić M, Bukurov M, Despotović B. 2022. Hydrothermal carbonization of agricultural biomass: Characterization of hydrochar for energy production. Solid Fuel Chem, 56: 225–235. DOI: 10.3103/S0361521922030077.

Petrovic´ JT, Stojanovic´ MD, Milojkovic´ JV, Petrovic´ MS, Šoštaric´ TD, Lauševic´ MD, Mihajlovic´ ML. 2016. Alkali modified hydrochar of grape pomace as a perspective adsorbent of Pb2+ from aqueous solution. J Environ Manage, 182: 292-300. DOI: 10.1016/j.jenvman.2016.07.081.

Pezoti O, Cazetta AL, Bedin KC, Souza LS, Martins AC, Silva TL, Júnior OOS, Visentainer JV, Almeida VC. 2016. NaOH-activated carbon of high surface area produced from guava seeds as a high-efficiency adsorbent for amoxicillin removal: Kinetic, isotherm and thermodynamic studies. Chem Eng J; 288: 778-788.

Qian K, Kumar A, Patil K, Bellmer D, Wang D, Yuan W, Huhnke RL. 2013. Effects of biomass feedstocks and gasification conditions on the physiochemical properties of char. Energies, 6 (8): 3972-3986. DOI: 10.3390/en6083972

Rashid RA, Jawad AH, Ishak MAM, Kasim NN. 2016. KOH-activated carbon developed from biomass waste: adsorption equilibrium, kinetic and thermodynamic studies for methylene blue uptake. Desalin Water Treat, 57:27226-27236. DOI: 10.1080/19443994.2016.1167630.

Redding AM, Cannon FS, Snyder SA, Vanderford BJ. 2009. A QSAR-like analysis of the adsorption of endocrine disrupting compounds, pharmaceuticals, and personal care products on modified activated carbons. Water Res, 43(15): 3849-3861. DOI: 10.1016/j.watres.2009.05.026.

Regmi P, Moscoso JLG, Kumar S, Cao X, Mao J, Schafran G. 2012.

Removal of copper and cadmium from aqueous solution using switchgrass biochar produced via hydrothermal carbonization process. J Environ Manage, 109: 61-69. DOI: 10.1016/j.jenvman.2012.04.047.

Rodrigues DLC, Machado FM, Osorio AG, Azevedo CFD, Lima EC, Silva RSD, Lima DR, FM Gonçalves. 2020. Adsorption of amoxicillin onto high surface area–activated carbons based on olive biomass: kinetic and equilibrium studies. Environ Sci Pollut Res, 27: 41394-41404. DOI: 10.1007/s11356-020-09583-6.

Roman S, Nabais JMV, Ledesma B, Gonzalez, JF, Laginhas C, Titrici MM. 2013. Production of low-cost adsorbents with tunable surface chemistry by conjunction of hydrothermal carbonization and activation processes. Microporous and Mesoporous Mater, 165: 127-133. DOI: 10.1016/j.micromeso.2012.08.006.

Satpathy SK, Tabil LG, Meda V, Naik SN, Prasad R, 2014. Torrefaction of wheat and barley straw after microwave heating. Fuel, 124: 269-278. DOI: 10.1016/j.fuel.2014.01.102.

Saucier C, Karthickeyan P, Ranjithkumar V, Lima EC, Dos Reis GS, De Brum IAS. 2017. Efficient removal of amoxicillin and paracetamol from aqueous solutions using magnetic activated carbon. Environ Sci Pollut Res, 2017, 24(6): 5918-5932. DOI:10.1007/s11356-016-8304-7.

Serna-Galvis EA, Ferraro F, Silva-Agredo J, Torres-Palma RA. 2017. Degradation of highly consumed fluoroquinolones, penicillins and cephalosporins in distilled water and simulated hospital wastewater by UV254 and UV254/persulfate processes. Water Res, 122: 128-138. DOI: 10.1016/j.watres.2017.05.065.

Sevilla M, Fuertes AB. 2011. Sustainable porous carbons with a superior performance for CO_2 capture. Energy Environ Sci, 4: 1765-71. DOI: 10.1039/C0EE00784F.

Sun K, Ro K, Guo M, Novak J, Mashayekhi H, Xing B. 2011. Sorption of bisphenol-A, alpha-ethinyl estradiol and phenanthrene on thermally and hydrothermally produced biochars. Biroresour Technol, 102: 5757-63. DOI: 10.1016/j.biortech.2011.03.038.

Swan NB, Zaini MAA. 2019. Adsorption of malachite green and congo red dyes from water: recent progress and future outlook. Ecol Chem Eng S, 26(1):119-132. DOI: 10.1515/eces-2019-0009.

Tran TH, Le HH, Pham TH, Nguyen DT, La DD, Chang SW, Lee SM, Chung,WJ, Nguyen DD. 2021. Comparative study on methylene blue adsorption behavior of coffee husk-derived activated carbon materials prepared using hydrothermal and soaking methods. J Environ Chem Eng, 9: 105362. DOI:10.1016/j.jece.2021.105362.

Unutkan T, Bakırdere S, Keyf S. 2018. Development of an analytical method for the determination of amoxicillin in commercial drugs and wastewater samples, and assessing its stability in simulated gastric digestion. J Chromatogr Sci, 56(1): 36-40. DOI: 10.1093/chromsci/bmx078.

Vassilev SV, Vassileva CG, Vassilev VS. 2015. Advantages and disadvantages of composition and properties of biomass in comparison with coal: An overview. Fuel, 158: 330-350, DOI:10.1016/j.fuel.2015.05.050.

Verma N, Bansal MC, Kumar V. 2011. Pea peel waste: a lignocellulosic waste and its utility in cellulase production by Trichoderma reesei under solid state cultivation. BioResource, 6: 1505-1519.

Wang T, Zhai Y, Zhu Y, Li C, Zeng G. 2018. A review of the hydrothermal carbonization of biomass waste for hydrochar formation: process conditions, fundamentals, and physicochemical properties. Renew Sustain Energy Rev, 90: 223–47. DOI: doi.org/10.1016/j.rser.2018.03.071.

Wu S, Wang Q, Cui D, Sun H, H Yin, Xu F, Wang Z. 2023. Evaluation of fuel properties and combustion behaviour of hydrochar derived from hydrothermal carbonisation of agricultural wastes, Journal of the Energy Institute, 108: 101209. DOI:10.1016/j.joei.2023.101209.

Yan W, Acharjee TC, Coronella CJ, Victor R, Vásquez VR. 2009. Thermal pretreatment of lignocellulosic biomass. Environ Prog Sustain Energy, 28: 435-440. DOI: 10.1002/ep.10385.

Yang X, Wan Y, Zheng Y, F He, Z Yu, Huang J, Wang H, YS Ok, Jiang Y, Gao B. 2019. Surface functional groups of carbon-based adsorbents and their roles in the removal of heavy metals from aqueous solutions: A critical review. Chem Eng J, 366: 608-621. DOI: 10.1016/j.cej.2019.02.119.

Yi H, Nakabayashi K, Yoon SH, Miyawaki J. 2021. Pressurized physical activation: A simple production method for activated carbon with a highly developed pore structure. Carbon, 183: 735-742. DOI: 10.1016/j.carbon.2021.07.061.

Yu F, Li Y, Han S, Ma J. 2016. Adsorptive removal of antibiotics from aqueous solution using carbon materials. Chemosphere, 153: 365-385. DOI: 10.1016/j.chemosphere.2016.03.083.

Zhu X, Liu Y, Qian F, Zhou C, Zhang S, Chen J. 2014. Preparation of magnetic porous carbon from waste hydrochar by simultaneous activation and magnetization for tetracycline removal. Bioresour Technol, 154: 209-214. DOI: 10.1016/j.biortech.2013.12.019.

Zuccato E, Castiglioni S, Bagnati R, Melis M, Fanelli R. 2010. Source, occurrence and fate of antibiotics in the Italian aquatic environment. J Hazard Mater, 179(1-3): 1042-1048. DOI: 10.1016/j.jhazmat.2010.03.110.